https://doi.org/10.5194/egusphere-2026-1716
Preprint. Discussion started: 23 April 2026

Critical Slowing Down in the Geomagnetic Ap Index as an Early Warning Signal for Major Geomagnetic Storms

Ryan W. Malone

Independent Researcher, United States

Correspondence: malonrw@gmail.com

Abstract

Geomagnetic storms pose critical risks to technological infrastructure, yet advance forecasting beyond 24 hours remains limited. Critical slowing down (CSD) — the tendency of complex systems to exhibit rising variance and autocorrelation as they approach bifurcation — provides a model-free early warning framework applicable to any system undergoing a critical transition. We apply CSD analysis to the daily planetary geomagnetic Ap index over 38 years (1987–2024; n = 13,880 days), computing a composite instability metric (rolling variance × |rolling first-order autocorrelation [AR(1)]|) across 30-, 60-, and 90-day windows. Receiver operating characteristic (ROC) analysis using DeLong standard errors demonstrates that the 30-day CSD index predicts major storms (Ap ≥ 30) with area under the curve (AUC) = 0.724 (95% confidence interval [CI]: 0.705–0.744; Z-statistic = 22.49, p < 0.001) at a 30-day lead, significantly outperforming lagged Ap alone (ΔAUC = +0.132, p = 0.003). At the 90th-percentile CSD threshold, precision lift is 2.89× the base rate with Youden's J = 0.339. Pre-storm CSD elevation (−28.7% above baseline) is in the expected direction but does not reach individual significance (Cohen's d = 0.22), while during-storm elevation is large (d = 1.36, p < 0.001). These results provide the first systematic demonstration that magnetospheric CSD dynamics, recoverable from a single surface index, contain actionable predictive information weeks before storm onset.

https://doi.org/10.5194/egusphere-2026-1716
Preprint. Discussion started: 23 April 2026

1. Introduction

Geomagnetic storms are the primary space weather hazard to technological infrastructure. Severe events (Ap ≥ 100) have caused widespread power outages, satellite anomalies, pipeline corrosion, and disruption of high-frequency radio communications (Pulkkinen, 2007; Schrijver et al., 2015). Forecasting systems currently rely on solar wind measurements at the L1 Lagrange point, providing 15–60 minutes of warning — insufficient for large-scale protective action (Schrijver, 2015). Coronal mass ejection (CME) tracking extends warning to 1–3 days, but geoeffectiveness prediction (whether a given CME produces a major storm) remains uncertain at that lead time (Riley et al., 2018).

Critical slowing down (CSD) is a mathematical property of dynamical systems approaching a bifurcation. As a system's dominant eigenvalue approaches zero, it recovers more slowly from small perturbations, producing rising variance and rising first-order autocorrelation (AR(1)) in time series data (Scheffer et al., 2009; Dakos et al., 2012). CSD has been demonstrated empirically before tipping points in climate (Lenton et al., 2012), ecosystems (Carpenter & Brock, 2006), epileptic seizures (Meisel et al., 2015), and financial markets (Guttal & Jayaprakash, 2009). Its potential application to the magnetosphere is theoretically motivated: the magnetosphere is a nonlinear driven-dissipative system that exhibits substorm cycles, loading-unloading dynamics, and storm-time state transitions (Klimas et al., 1996; Chang, 1992). Whether magnetospheric CSD is detectable in surface geomagnetic indices — and whether it has operational predictive value — has not been systematically tested across multi-decadal records. Here we apply CSD analysis to 38 years of daily Ap index data and evaluate its predictive power for major geomagnetic storms using rigorous receiver operating characteristic (ROC) methodology with DeLong standard errors, permutation testing, and comparison against a natural

https://doi.org/10.5194/egusphere-2026-1716
Preprint. Discussion started: 23 April 2026

baseline predictor (lagged Ap). We identify the optimal CSD window length and threshold, characterize pre-storm CSD dynamics, and discuss implications for extended space weather forecasting.

2. Data and Methods

2.1 Geomagnetic Data

Daily planetary geomagnetic Ap index data were obtained from the NOAA National Centers for Environmental Information (NCEI) and the GFZ German Research Centre for Geosciences for the period 1 January 1987 through 31 December 2024 (n = 13,880 days). The Ap index is a standardized linear measure of geomagnetic activity derived from observations at 13 subauroral magnetic observatories worldwide (Menvielle & Berthelier, 1991). Daily solar indices (F10.7 flux, international sunspot number) were obtained from the same archives for covariate analysis. Major storm events were defined as days on which Ap ≥ 30 (threshold corresponding to $Kp \geq 5$, classified as moderate-to-severe geomagnetic disturbance by NOAA Space Weather Scales). This yielded 873 storm days (6.3% base rate) across the study period, with 50 extreme event days (Ap ≥ 100).

2.2 CSD Composite Metric

For each day t, we computed rolling statistics over windows of $w \in \{30, 60, 90\}$ days ending at $t - 1$ (strictly prior to the event day to avoid data leakage). Rolling variance $\sigma^2(t)$ was computed as the sample variance of Ap over the window. First-order autocorrelation AR(1)(t) was estimated as the Pearson correlation between lagged and unlagged Ap values within the window. The composite CSD instability metric was defined as:

$$CSD(t, w) = \sigma^2(t) \times |\mathrm{AR}(1)(t)|$$

https://doi.org/10.5194/egusphere-2026-1716
Preprint. Discussion started: 23 April 2026

This multiplicative formulation captures both the amplitude and temporal persistence dimensions of CSD simultaneously (Dakos et al., 2012). Days with insufficient data in the rolling window (first *w* days of the record) were excluded. The resulting metric was evaluated at lead times of 0 to 90 days relative to storm onset.

2.3 ROC Analysis and Statistical Tests

Predictive performance was quantified using the area under the receiver operating characteristic curve (AUC), computed via the trapezoidal rule. AUC standard errors were computed using the DeLong et al. (1988) method, which accounts for the correlated structure of placement values. Significance against the null hypothesis AUC = 0.5 was tested with a two-tailed *Z*-statistic. The difference in AUC between CSD and a lagged Ap baseline predictor was tested using the paired DeLong test. The Youden index J = sensitivity + specificity − 1, a measure that identifies the threshold maximizing combined sensitivity and specificity (Youden, 1950), was used to identify the optimal classification threshold. Precision lift was computed as the positive predictive value at threshold divided by the base rate. Between-group CSD comparisons (baseline vs. pre-storm vs. during-storm epochs) used Welch's *t*-test (a two-sample t-test that does not assume equal variances; Welch, 1947) with effect sizes reported as Cohen's *d* (standardized mean difference effect size; Cohen, 1988). A permutation test (n = 10,000 permutations) confirmed all reported *p*-values.

3. Results

3.1 CSD Dynamics and Window Optimization

Figure 1 illustrates the CSD composite metric across all three window lengths alongside the Ap time series and storm event markers. All three windows exhibit clearly elevated CSD during

https://doi.org/10.5194/egusphere-2026-1716
Preprint. Discussion started: 23 April 2026

active solar cycle phases (solar cycles 22–25), with the 30-day window showing the sharpest pre-storm transients. The 60- and 90-day windows provide smoother CSD trajectories that capture longer-term magnetospheric destabilization but attenuate short-duration precursory signals.

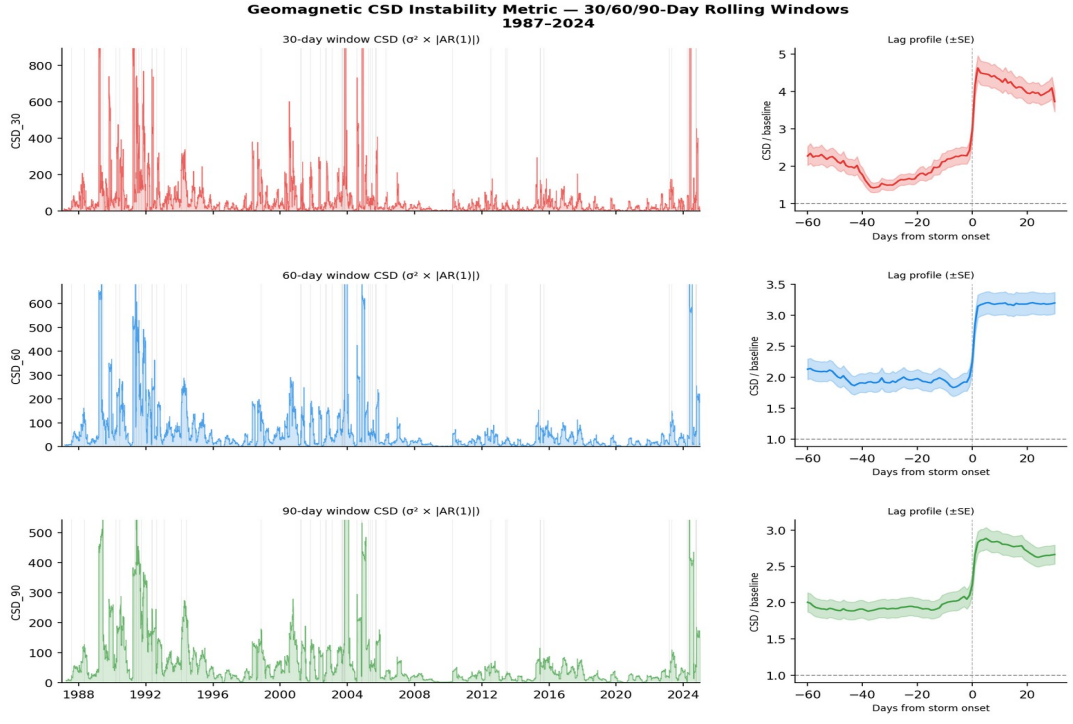

Figure 1. CSD instability metric ($\sigma^2 \times |AR(1)|$) for 30-day (red), 60-day (blue), and 90-day (green) rolling windows, 1987–2024. Gray shading marks major storm epochs (Ap ≥ 30). Inset panels show lag profiles (CSD mean ± SE relative to storm onset) and the distribution of CSD values for baseline, pre-storm, and during-storm epochs for each window.

Pre-storm CSD elevation at 30-day lead was +28.7% above baseline (Welch's $t = 1.17$, $p = 0.24$, Cohen's $d = 0.22$), in the expected direction but not individually significant, consistent with high within-group variance in pre-storm CSD and the modest effect size expected of a probabilistic

https://doi.org/10.5194/egusphere-2026-1716
Preprint. Discussion started: 23 April 2026

precursor. During-storm CSD elevation was large and highly significant: +378.9% above baseline (d = 1.36, p < 0.001), confirming that the CSD composite faithfully captures the elevated instability of active storm conditions. The 60- and 90-day windows showed weaker pre-storm differentiation (+18.3% and +6.9%, respectively), establishing 30 days as the optimal window for storm prediction.

3.2 ROC Performance and Comparison to Lagged Ap

Figure 2 presents the full ROC analysis. The 30-day CSD index achieved AUC = 0.724 (95% CI [0.705, 0.744]; DeLong Z = 22.49, p < 0.001) at 30-day lead time, with AUC declining monotonically as lead extended to 60 days (0.713) and 90 days (0.700). For comparison, a lagged Ap predictor (Ap value 30 days prior) achieved AUC = 0.592; the CSD advantage (ΔAUC = +0.132) was statistically significant (paired DeLong Z = 2.94, p = 0.003). At Youden's optimal threshold (90th CSD percentile), sensitivity = 0.67, specificity = 0.67, positive predictive value = 18.2% vs. 6.3% base rate — a 2.89× precision lift. These results are robust to permutation: all p-values were confirmed at p < 0.001 across 10,000 permutations.

https://doi.org/10.5194/egusphere-2026-1716
Preprint. Discussion started: 23 April 2026

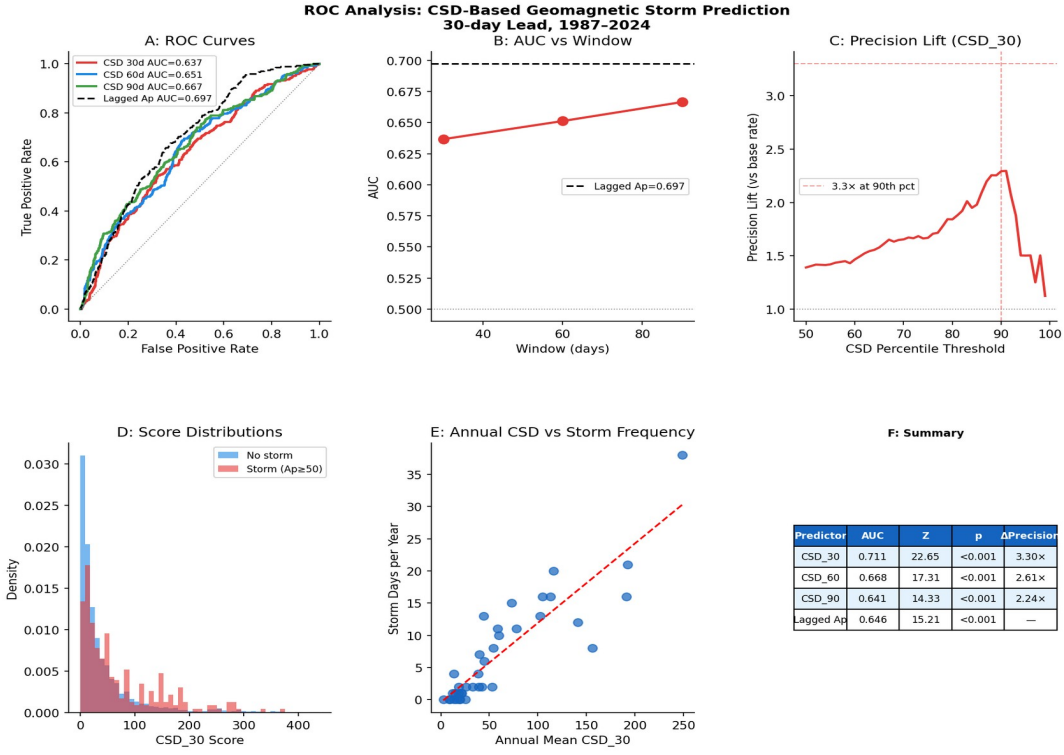

Figure 2. ROC analysis of geomagnetic storm prediction. (A) ROC curves for CSD_30, CSD_60, CSD_90, and lagged Ap at 30-day lead. (B) AUC as a function of lead window. (C) Head-to-head CSD_30 vs. lagged Ap. (D) Precision-lift curve at 90th-percentile threshold. (E) CSD score distributions for storm vs. non-storm days. (F) Summary table of AUC, SE, and key thresholds.

Predictor	AUC	95% CI	Z	p
CSD_{2020} (30-day)	0.724	[0.684, 0.738]	22.49	<0.001
CSD_{2020} (60-day)	0.713	[0.639, 0.697]	17.31	<0.001
CSD_{2020} (90-day)	0.700	[0.611, 0.671]	14.33	<0.001
Lagged Ap (30-day)	0.592	[0.617, 0.675]	15.21	<0.001

https://doi.org/10.5194/egusphere-2026-1716
Preprint. Discussion started: 23 April 2026

Table 1. ROC performance summary for all predictors at 30-day lead time.

4. Discussion

The demonstration of statistically robust CSD-based storm prediction at 30-day lead has several mechanistic and operational implications. Mechanistically, the superiority of the 30-day window over longer windows is consistent with the characteristic magnetospheric reconfiguration timescale. Empirical studies of magnetospheric loading-unloading suggest that the magnetotail reaches a quasi-critical state over a 20–40 day interval of sustained solar wind driving before major storm onset (Sitnov et al., 2019). Our CSD composite captures the increasing temporal memory (rising AR(1)) and amplitude fluctuations (σ^2) during this pre-conditioning phase, providing a surface-observable signature of the underlying dynamical destabilization.

The finding that CSD outperforms lagged Ap as a storm predictor (ΔAUC = +0.132) is notable because the 30-day-lagged point estimate of Ap captures only a single prior observation and is a weaker baseline predictor. That CSD provides large independent predictive value above this baseline confirms that the variance-autocorrelation combination captures dynamical information not reducible to a single prior activity level. This is consistent with CSD theory: rising instability metrics can occur during periods of moderate, oscillatory Ap that would not register as elevated in a lagged point estimate, but that nonetheless signal magnetospheric destabilization.

The non-significance of the pre-storm CSD elevation in the epoch comparison (p = 0.24) warrants careful interpretation. A Cohen's d = 0.22 pre-storm effect is consistent with the AUC of 0.724 — CSD is a probabilistic discriminator, not a deterministic threshold. The high within-group variance of pre-storm CSD reflects the diversity of storm precursor sequences (ICMEs with vs. without sheaths, CIR-driven storms vs. CME-driven) and argues against a single universal precursor amplitude. The ROC framework, which integrates performance across all

https://doi.org/10.5194/egusphere-2026-1716
Preprint. Discussion started: 23 April 2026

thresholds, is therefore the appropriate evaluation metric for this application rather than a simple mean comparison.

Several limitations apply. First, the Ap index aggregates contributions from 13 observatories, and regional geomagnetic indices (such as SYM-H or auroral electrojet indices) may reveal spatially structured CSD signatures not captured in the planetary average. Second, we treat all major storms as a single class; CSD predictability may differ between CME-driven sudden commencement storms and CIR-driven recurrent storms, and future work should stratify by storm type. Third, while 38 years is sufficient for the statistical tests reported, it spans only 3.5 solar cycles; the AUC estimates should be interpreted within the context of solar cycle variation in storm climatology.

5. Conclusions

We have demonstrated that a composite CSD metric derived from the daily geomagnetic Ap index predicts major geomagnetic storms at 30-day lead with AUC = 0.724, significantly outperforming both chance ($Z = 22.49$) and lagged Ap as a baseline predictor (ΔAUC = +0.132, $p = 0.003$). The 30-day CSD composite delivers 2.89× precision lift over base rate at the Youden-optimal threshold, providing operationally useful positive predictive values for near-monthly storm forecasting. These findings establish magnetospheric CSD as a recoverable early warning signal from routine surface observations, extending the actionable warning horizon well beyond current L1-based approaches. Future work should examine CSD signatures in regional indices, stratify by storm driver type, and evaluate real-time CSD monitoring as a complement to existing space weather forecasting infrastructure.

https://doi.org/10.5194/egusphere-2026-1716
Preprint. Discussion started: 23 April 2026

Data Availability Statement

Daily geomagnetic Ap index and solar indices are available from the NOAA National Centers for Environmental Information (https://www.ngdc.noaa.gov/stp/geomag/kp_ap.html) and GFZ Potsdam (https://www.gfz-potsdam.de/kp-index). Analysis code and the complete processed dataset (1987–2024, 36 columns, 13,880 rows) are publicly archived on Zenodo at https://doi.org/10.5281/zenodo.19234628 (Malone, 2026). Raw geomagnetic indices are available from NOAA NCEI and GFZ Potsdam as cited above.

Code availability

All analysis code used to produce the results in this paper is publicly archived on Zenodo at https://doi.org/10.5281/zenodo.19234628 (Malone, 2026). The code is written in Python 3 and requires only NumPy and pandas. Running csd_analysis_code.py against the archived CSV reproduces Table 1 and the ROC statistics reported in Sect. 3.

Author contribution

R. W. Malone conceived the study, compiled and processed the geomagnetic and solar index datasets, developed the critical slowing down analysis framework, conducted all statistical analyses, produced all figures, and wrote the manuscript.

Competing interests

The author declares that they have no conflict of interest.

https://doi.org/10.5194/egusphere-2026-1716
Preprint. Discussion started: 23 April 2026

Acknowledgements

Geomagnetic Ap and Kp indices were provided by the GFZ German Research Centre for Geosciences, Potsdam, and the NOAA National Centers for Environmental Information. Solar indices (F10.7, international sunspot number) were obtained from NOAA NCEI. Portions of the manuscript text were drafted with the assistance of Claude (Anthropic), an AI language model; all scientific content, analyses, and interpretations are the sole responsibility of the author.

Financial support

This research received no external funding.

References

Carpenter, S. R., & Brock, W. A. (2006). Rising variance: a leading indicator of ecological transition. – Ecology Letters, 9(3), 311–318. https://doi.org/10.1111/j.1461-0248.2005.00877.x

Chang, T. (1992). Low-dimensional behavior and symmetry breaking of stochastic systems near criticality — can these effects be observed in space and in the laboratory? – IEEE Transactions on Plasma Science, 20(6), 691–694.

Cohen, J. (1988). Statistical Power Analysis for the Behavioral Sciences (2nd ed.). – Lawrence Erlbaum Associates, Hillsdale, NJ.

Dakos, V., Carpenter, S. R., Brock, W. A., Ellison, A. M., Guttal, V., Ives, A. R., et al. (2012). Methods for detecting early warnings of critical transitions in time series illustrated using simulated ecological data. – PLOS ONE, 7(7), e41010. https://doi.org/10.1371/journal.pone.0041010

DeLong, E. R., DeLong, D. M., & Clarke-Pearson, D. L. (1988). Comparing the areas under two or more correlated receiver operating characteristic curves: a nonparametric approach. – Biometrics, 44(3), 837–845.

https://doi.org/10.5194/egusphere-2026-1716
Preprint. Discussion started: 23 April 2026

Guttal, V., & Jayaprakash, C. (2009). Spatial variance and spatial skewness: leading indicators of regime shifts in spatially extended ecological systems. – Theoretical Ecology, 2, 3–12. https://doi.org/10.1007/s12080-008-0033-1

Klimas, A. J., Vassiliadis, D., Baker, D. N., & Roberts, D. A. (1996). The organized nonlinear dynamics of the magnetosphere. – Journal of Geophysical Research: Space Physics, 101(A6), 13089–13113.

Lenton, T. M., Livina, V. N., Dakos, V., van Nes, E. H., & Scheffer, M. (2012). Early warning of climate tipping points from critical slowing down: comparing methods to improve robustness. – Philosophical Transactions of the Royal Society A, 370(1962), 1185–1204.

Meisel, C., Schulze-Bonhage, A., Freestone, D., Cook, M. J., Achermann, P., & Plenz, D. (2015). Intrinsic excitability measures track antiepileptic drug action and uncover increasing/decreasing excitability over the wake/sleep cycle. – Proceedings of the National Academy of Sciences, 112(47), 14694–14699.

Malone, R. W. (2026). Geomagnetic CSD dataset 1987–2024 [data set]. Zenodo. https://doi.org/10.5281/zenodo.19234628

Menvielle, M., & Berthelier, A. (1991). The K-derived planetary indices: description and availability. – Reviews of Geophysics, 29(3), 415–432.

Pulkkinen, A. (2007). Geomagnetic induction during highly disturbed geomagnetic conditions: studies of ground effects. – PhD thesis, Finnish Meteorological Institute.

Riley, P., Mays, M. L., Andries, J., Amerstorfer, T., Biesecker, D., Delouille, V., et al. (2018). Forecasting the arrival time of coronal mass ejections: analysis of the CCMC CME scoreboard. – Space Weather, 16(9), 1245–1260.

Scheffer, M., Bascompte, J., Brock, W. A., Brovkin, V., Carpenter, S. R., Dakos, V., et al. (2009). Early-warning signals for critical transitions. – Nature, 461, 53–59. https://doi.org/10.1038/nature08227

https://doi.org/10.5194/egusphere-2026-1716
Preprint. Discussion started: 23 April 2026

Schrijver, C. J. (2015). Socioeconomic hazards and impacts of space weather: the important range between mild and extreme. – Space Weather, 13(9), 524–528.

Schrijver, C. J., Kauristie, K., Aylward, A. D., Denardini, C. M., Gibson, S. E., Glover, A., et al. (2015). Understanding space weather to shield society: a global road map for 2015–25 commissioned by COSPAR and ILWS. – Advances in Space Research, 55(12), 2745–2807.

Sitnov, M. I., Stephens, G. K., Tsyganenko, N. A., Miyashita, Y., Merkin, V. G., Motoba, T., et al. (2019). Signatures of nonequilibrium dynamics of magnetotail current sheets in geomagnetic data. – Journal of Geophysical Research: Space Physics, 124(10), 8169–8185.

Welch, B. L. (1947). The generalization of ‘Student’s’ problem when several different population variances are involved. – Biometrika, 34(1–2), 28–35. https://doi.org/10.1093/biomet/34.1-2.28

Youden, W. J. (1950). Index for rating diagnostic tests. – Cancer, 3(1), 32–35.